PHYSICAL REVIEW B VOLUME 24, NUMBER 2 15 JULY 1981

Lattice distortion and volume change in a dilute heterovalent alloy: *Al*Li

G. Solt
Institute of Theoretical Physics, University of Lausanne, CH-1015 Lausanne, Switzerland

K. Werner
Institut für Festkörperforschung, Kernforschungsanlage Jülich, D-5170 Jülich, Germany
(Received 15 October 1980)

A theoretical and experimental study of the lattice strain and volume change in the dilute solid solution *Al*Li is presented. The experimental data were obtained by diffuse elastic neutron scattering in Al single crystals containing 0.26 and 0.88 at. % ^{7}Li, respectively. The isotope ^{7}Li was used because of the small absorption and the known incoherent cross section of this nucleus. The theoretical method to calculate the volume change, the lattice distortion, and the heat of solution for a heterovalent substitutional impurity is developed within the framework of the perturbed electron-liquid pseudopotential formalism. It is shown that in determining the long-range part of the lattice displacement in a heterovalent dilute alloy such as *Al*Li, third- and fourth-order nonlinear screening contributions to the distorting force are equally significant in addition to the traditional linear screening term. This is in contrast to the case of a homovalent solution, where fourth-order nonlinear screening can be ignored. The numerical calculation is based on the ion-electron potentials for pure Al and Li that have been determined by using lattice-constant and elastic or phonon data for each of the pure constituents. The agreement is reasonably good with both the observed anomalous, negative volume change and with the measured lattice strain. The inadequacy of Vegard's rule to predict even the sign of the volume change in this alloy is discussed.

I. INTRODUCTION

Point defects (impurities, vacancies) in a metallic matrix cause a perturbation of the system which is due to the different ion-electron interaction and, as a consequence, the different electron distribution in the neighborhood of the defect. The response of the lattice consists in establishing new equilibrium positions of the surrounding host atoms, involving also a new average lattice spacing for the whole system.

A detailed knowledge of the static distortion field induced by the defect gives information about the nature and range of the forces between the ions, which in a metal are interactions via the polarized electron liquid, and can lead to a better understanding of the mechanism of alloy formation. Therefore, in addition to measuring the average volume change associated with the defect which, as in the case of the dilute Al-Li system, may give already interesting or even paradoxical results,[1,2] the study of the *details* of the displacement field by scattering methods has also been the subject of extensive theoretical and experimental investigation.[3]

A most important experimental technique to observe the defect-induced distortion in a host matrix is the diffuse elastic scattering of neutrons.[3,4] In this method the intensity of neutrons of an incoming wavelength of 0.3–0.8 nm scattered by a single crystal containing the defects is observed as a function of momentum transfer $\vec{q}$. Using a multidetector machine with energy analysis, it is possible to separate the inelastic and elastic scattering and determine the diffuse elastic cross section fairly accurately, with a total error of less than 5% for the resulting values of the distortion field. The possible range of the momentum transfer for the experimental setup[4] at the reactor in Jülich, at which the present measurements were done, reaches from about 1 nm^{-1} to about 35 nm^{-1}, corresponding, in real space, to the distances of 0.2–6 nm from the impurity, i.e., from nearest neighbors up to atoms within 5–10 lattice spacings. The main body of the present work is the description and the theoretical analysis of the results obtained by this scattering technique.

From the theoretical point of view, the distortion around an impurity can easily be calculated by the now standard method of lattice statics, described, e.g., in Ref. 3, provided both the dynamics of the pure solvent crystal *and* the distorting forces arising from the presence of the solute atom are known. While in earlier work phenomenological force-constant models were used to represent the interaction between host and impurity atoms, the development of the pseudopotential theory[5] has made it possible, for simple metals, to eliminate this "*ad hoc*" approach and replace it by "*ab initio*" calculations, as was the case before with the lattice dynamics[6] of pure nontransition metals. Thus, the electron-liquid pseudopotential formalism was applied to calculate the distortion due to a vacancy and also to substitutional impurities of the same valence as the host atoms,[7-10] and the problem connected with the convergence of the

pseudopotential expansion and nonlinear screening has, for such homovalent impurities, also been clarified.[9] This is, however, not the case for a *heterovalent* impurity. Although the neutron scattering method has been applied with success to measure the lattice strain[11] in *Al*Mg and a preliminary analysis has been given for those results, the systematic study of the pseudopotential method in the context of calculating the equilibrium cohesive parameters for a heterovalent solute has not, to our knowledge, been given previously.

In the present work the theoretical method to calculate cohesive properties, such as the average lattice spacing, individual atomic displacements, and heat of solution, is developed for a dilute substitutional alloy with difference in valency between solute and solvent, and the formalism is applied to the alloy *Al*Li for which the scattering experiment has been performed. Special attention is paid to the observed volume contraction in this alloy, a striking and long known example where the interpolation scheme (Vegard's rule) does not give even the correct *sign* for the variation of the lattice spacing, and to the contribution of nonlinear screening of the electrons in determining the atomic displacements in the preasymptotic and asymptotic range.

In Sec. II the experimental procedure is described, including the preparation of the single crystal *Al*Li sample, the neutron scattering setup, and the data processing which leads to the value of the cross section of coherent scattering at the lattice strain.

In Sec. III the theory is developed within the framework of the perturbed electron-liquid pseudopotential formalism. The total energy of the lattice with impurity is expressed as a perturbation series in ascending powers of the *ion-electron potentials* with arbitrary positions of the host atoms. Rearranging this series corresponding to ascending powers of the *atomic displacements*, we obtain first a term referring to an undistorted lattice, ΔE_{per}, which can be used to derive the average lattice spacing in the alloy. Next, the linear term of the expansion gives the distorting force $\vec{f}(\vec{l})$, and the static displacements can then be determined by the well known method of lattice statics. The new theoretical result concerns, first of all, the long-range part of the displacement field and the volume change. For a homovalent alloy it has previously been shown[9] that, in calculating the static displacements $\vec{u}(\vec{q})$ by the above method, the perturbation series in terms of the ion-electron interactions is not "uniformly convergent," namely, that for $|\vec{q}| \ll |\vec{G}|$ the third-order nonlinear screening term becomes of the same order of magnitude as the linear screening contribution. It was also shown that, as a consequence, a discrepancy arises between the volume change derived from ΔE_{per} and the long-range behavior of the displacement field every time when both these quantities are calculated in the linear screening approximation.

A more general result is derived here for the heterovalent alloy, containing as a special case the above statement for the homovalent solution. We show that in the case of a difference in valency, *both* third- and fourth-order nonlinear screening terms are appreciable in calculating the displacements outside the immediate vicinity of the solute atom. The *fourth*-order term is found to be *linear* in the valence difference and that is why it does not appear in the homovalent case.

The results show that the volume change per solute atom and, hence, the *asymptotic* amplitude of the displacement field can, nevertheless, be calculated by the linear screening approximation via ΔE_{per}, but the necessity of an explicit calculation of third- and fourth-order screening terms arises for the Fourier components of the displacement field in the range $0 < |\vec{q}| \ll |\vec{G}|$.

The numerical results, described in Sec. IV, are *"ab initio"* in the sense that the input data concerning the ion-electron potentials for solvent and solute have been fixed *without* using information on the properties of the alloy, by fitting the cohesive parameters of the *pure* constituents. The results for the predicted volume change are fairly reasonable; both the observed negative sign and the anomalously small magnitude of $\Delta\Omega_0$ are reproduced. The volume *contraction* observed[1,2] in Al on dissolving Li atoms has always been considered as paradoxical, since the Wigner-Seitz cell of Li is considerably *larger* than that of the solvent aluminium. Apart from some general, qualitative arguments[1] invoked by Axon and Hume-Rothery, the present treatment seems to be the first quantitative analysis for the volume change in this alloy. The present experimental data, mapping the displacement field around the solute atom, are in reasonable agreement with the theory for both screening approximations used in the treatment. The nonlinear screening contribution to the asymptotic amplitude of displacement field is appreciable in both cases and implies a particularly drastic change of the scattering cross section for the Geldart-Vosko dielectric function. The heat of solution ΔH_s is also evaluated and the role of the different contributions is analyzed. Section V contains the conclusions.

II. EXPERIMENTAL

A. The Al-Li system

As a candidate for an experimental and theoretical study of the lattice distortion caused by a so-

lute atom, the dilute alloy *Al*Li has several advantages. As obvious requirements for such a system we have the following: (a) random distribution of the impurity atoms, (b) sufficiently large difference in scattering lengths of host and impurity nuclei, (c) well known and possibly small incoherent cross sections, and (d) weak absorption. Further, if (e) the difference in size between host and impurity atoms is not too large so that the displacements are small and (f) both components are simple *s-p* metals, a first-principle theoretical treatment based on the electron-liquid pseudopotential method is reasonably simple. These conditions are all met for the aluminum-lithium solid solution.

The Al-rich part of the phase diagram[12] is shown in Fig. 1. The α phase has the fcc structure of pure aluminum. The four circles mark the temperature-concentration parameters for which the measurements were performed. As there was no difference in the scattering pictures obtained at different samples and at different temperatures, we take this as experimental evidence that no concentration fluctuation connected with ordering occurs in the sample and that the distribution of the lithium impurities is random.

For the coherent scattering lengths we have[13]

$$b_{\mathrm{Al}} = (0.3449 \pm 0.0012) \times 10^{-12} \text{ cm},$$

$$b_{(^7\mathrm{Li})} = -(0.233 \pm 0.003) \times 10^{-12} \text{ cm},$$

and ^{7}Li was used since for this isotope (i) the absorption cross section is small, (ii) the incoherent cross section is known, and (iii) the coherent scattering length is large and opposite in sign to that of the Al nucleus. The advantage of the large negative scattering length becomes clear when we look at the cross section related to the lattice distortion, Eq. (3) in Sec. III, showing that the intensity of this scattering is proportional to the difference in scattering lengths of host and impurity.

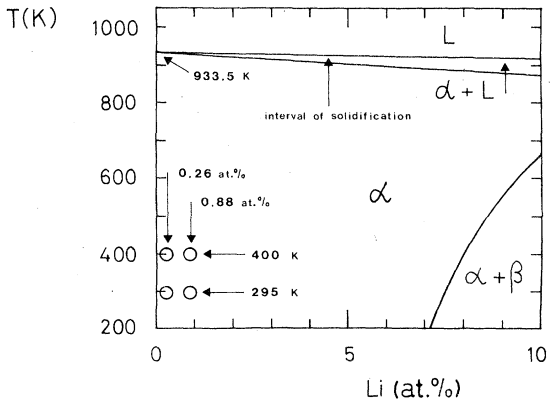

FIG. 1. Phase diagram (Ref. 12) for the Al-Li system in the aluminum-rich region. The α phase has fcc structure. The circles show the concentration and temperature parameters for which the experiment was performed.

Further, the incoherent cross section of Al is fairly small, and though this is not the case with the solute ^{7}Li, the *total* incoherent scattering is still small. As to point (d), the absorption is indeed very low, less than 5% for the samples used in the experiment (diameter $\simeq$20 mm). The fulfillment of the "theoretical" requirements (e) and (f) will be discussed in detail.

B. Sample preparation

Using Al of 99.9999% purity and ^{7}Li isotope of 99.95% purity (containing more than 0.04% of ^{6}Li), the alloys were prepared in a pure argon atmosphere. The nominal ^{7}Li concentrations were 2 and 3.5 at.%, respectively. A chemical analysis of small pieces after alloying yielded exactly these values. Single crystals were grown from the alloy in a Bridgman furnace with the ⟨110⟩ direction parallel to the cylinder axis. We used BN crucibles under 2-kbar Ar pressure. The crystals had a diameter of 20 mm and a length of 150 mm. Because of the high diffusion rate of Li in Al, large concentration losses occurred. Moreover, as seen in Fig. 1, the crystallization takes place in an interval of solidification, implying that a concentration gradient appears along the crystal axis. Chemical analysis gave values from 240 at.ppm at the lower part of the crystal up to 1.65 at.% at the upper end. Out of several crystals so grown we chose those with the smallest concentration gradients. From spark analysis on the crystals we found that the gradient Δc followed very well the equation[14]

$$\Delta c = K c_0 (1-g)^{k-1},$$

where c_0 means the nominal concentration and g is the reduced length of the crystal, while $k = c_s/c_e$ is the quotient of the solid and liquid concentration at a fixed temperature. Using the results of the chemical analysis together with the above equation, the mean concentrations of the two crystals chosen for the experiment were 0.88 and 0.26 at.%. In addition, a pure Al single crystal of the same dimensions as the *Al*Li crystals was also grown. The difference of the scattering intensities from the alloy and from the pure host is used to obtain the scattering in the lattice strain, as shown in the next paragraph. The rocking curves of the crystals, determined by a γ diffractometer, were about equal and of the magnitude 5′ to 10′.

C. Determination of the diffuse elastic neutron cross section

The experiments were performed at the *DNS*1 spectrometer[4] of the KFA in Jülich. The neutrons, moderated in a cold source, reach a velocity selector; the wavelength selected for our experiment was 0.44 nm, $\Delta\lambda/\lambda$ being 17%. Passing a Fermi chopper, the neutrons are scattered by the sample, which is adjusted in the center of the spectrometer table in an evacuated furnace. The scattered intensity is registered by 32 BF_3 counters at a radius of 80 cm around the sample, the angle range being 6° to 147°. For the above value of λ this means a range of momentum transfer from 2 to 25 nm^{-1}. Time-of-flight analysis was applied to separate the elastically scattered intensity.

The measurements were done on both *Al*Li crystals at temperatures of 295 and 400 K by rotating the samples in the beam in steps of 5°. After each run the intensity of the pure Al crystal was determined. In Fig. 2, the time-of-flight spectra of the *Al*Li sample containing 0.88 at.% Li and the pure-Al sample for the corresponding orientation are shown. One notices that the inelastic intensities are the same, and the difference in the elastic line is due to the Laue scattering and to the scattering on the lattice strain which we are looking for. To gain absolute values of the cross section, a vanadium calibration was carried out. The cross section for the diffuse elastic scattering—corrected for the Debye-Waller factors—is found as

$$\frac{d\sigma}{d\vec{\Omega}} = \frac{1}{c}\left(\frac{d\sigma}{d\vec{\Omega}}\right)^{V}_{\text{inc}} \frac{\dot{Z}_{\text{AlLi}}\exp(+2W_{\text{AlLi}}) - \dot{Z}_{\text{Al}}\exp(+2W_{\text{Al}})}{\dot{Z}_{V}\exp(+2W_{V}) - \dot{Z}_{B}}\,\Lambda - \left(\frac{d\sigma}{d\vec{\Omega}}\right)^{\text{Li}}_{\text{inc}}, \tag{1}$$

with

$$\Lambda = \frac{\rho_V}{A_V}\Big/\frac{\rho_{\text{Al}}}{A_{\text{Al}}} = 1.19$$

as a correction factor for having the same number of scattering atoms in the sample and the vanadium standard. Further, $\dot{Z}_{\text{AlLi}}$, $\dot{Z}_{\text{Al}}$, $\dot{Z}_V$, and $\dot{Z}_B$ are the counting rates in the elastic line of the sample, the Al crystal, the V standard, and the background, respectively. For the incoherent cross section of ^{7}Li we have[15]

$$\left(\frac{d\sigma}{d\vec{\Omega}}\right)^{\text{Li}}_{\text{inc}} = (47 \pm 3)\ \text{mb/sr},$$

whereas for vanadium the known value

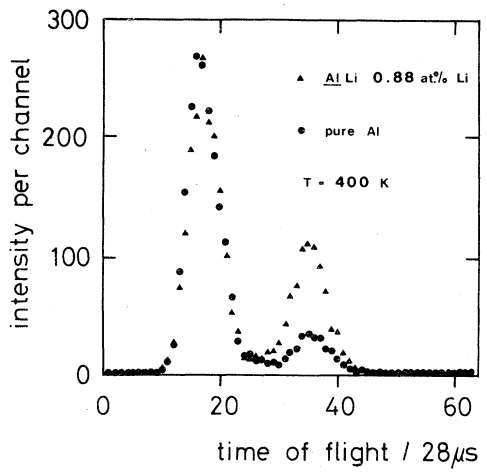

FIG. 2. Time-of-flight spectra of the *Al*Li sample (0.88 at.% Li) and that of pure Al for $|\vec{q}| = 1.18$ Å^{-1}. The difference in the elastic line is due to the difference in scattering lengths and to the lattice strain, according to Eq. (3). The inelastic spectra are seen not to differ appreciably.

$$\left(\frac{d\sigma}{d\vec{\Omega}}\right)^{V}_{\text{inc}} = (403.5 \pm 6.1)\ \text{mb/sr}$$

was used.

Supposing $W_{\text{AlLi}} \approx W_{\text{Al}}$ and neglecting the temperature dependence of Z_B ($Z_B \approx 10^{-3} Z_V$), the quotient $\exp(+2W_{\text{Al}})/\exp(+2W_V)$ is factored out. The Debye-Waller factors are calculated in a Debye approximation with $\Theta_{\text{Al}} = 342$ K, the values for W_{AlLi} and W_{Al} are set equal. Even for the largest $|\vec{q}|$ values measured, the influence of the Debye-Waller factor turned out to be less than 5% on the counting rates. The results for the mean symmetry directions ⟨110⟩, ⟨100⟩, and ⟨111⟩ are discussed in Sec. IV. Here we mention only that at two $\vec{q}$ values the measured cross section, as obtained via Eq. (1), could be directly checked, namely at $\vec{q} \approx 0$ and at $\vec{q} = \frac{1}{2}\vec{G}$, where $\vec{G}$ is any reciprocal-lattice vector. In the case of $\vec{q} = \frac{1}{2}\vec{G}$ we have pure Laue scattering[16] and the contribution of the lattice distortion vanishes, therefore with the scattering lengths, quoted in Sec. II A, we have

$$\left(\frac{d\sigma}{d\vec{\Omega}}\right)_{\vec{q}=(1/2)\vec{G}} = |b_{\text{Al}} - b_{\text{Li}}|^2 = (334 \pm 1)\text{mb}/(\text{sr at.\% solute}). \tag{2}$$

On the other hand, near $\vec{q} = 0$ the intensity can be expressed in terms of the elastic constants and the change in the average lattice spacing, as discussed later in Secs. III and IV. The agreement between the experimental values obtained via Eq.

(1) and by the two independent calculations of the cross section, at $\vec{q}=0$ and $\vec{q}=\frac{1}{2}\vec{G}$, is very convincing, as seen explicitly in Fig. 4. In this same figure we can see that the experimental errors are small compared to the resolved structure in the intensity distribution.

III. THEORETICAL

A. The scattering intensity

For the differential cross section of coherent diffuse elastic neutron scattering by an ideally disordered substitutional solid solution, obtained experimentally via Eq. (1), we have[3,4]

$$\frac{d\tilde{\sigma}}{d\vec{\Omega}} \equiv Nc\,\frac{d\sigma}{d\vec{\Omega}} = Nc\,|b_i - b + bK(\vec{q})|^2 , \tag{3}$$

where N is the total number of the scattering atoms and c is the concentration of the solute. This formula holds for $c \ll 1$. The Debye-Waller factors multiplying the b's are left out in Eq. (3), since we compare with the experimental value Eq. (1), corrected for this $\vec{q}$ dependence; $\vec{q}=\vec{k}-\vec{k}_0$ is the change in wave vector of a neutron scattered from the direction $\hat{k}_0$ into $\hat{k}$, and the function $K(\vec{q})$ is the scattering amplitude due to the displacement field around *one single* solute atom. The lattice is supposed to have one atomic site per unit cell. The position vector $\vec{R}(\vec{l})$ of each solvent atom in the alloy can be written as

$$\vec{R}(\vec{l}) = \vec{l} + \vec{u}(\vec{l}) , \tag{4}$$

where $\vec{l}$ is the position of the lattice site in the *undistorted* host crystal and $\vec{u}(\vec{l})$ stands for the static displacement due to the presence of the impurity. The amplitude of scattering on the lattice strain is given by

$$K(\vec{q}) = -i\vec{q}\cdot\vec{u}_{\vec{q}} , \tag{5a}$$

where

$$\vec{u}_{\vec{q}} = \sum_{\vec{l}} \vec{u}(\vec{l})e^{-i\vec{q}\cdot\vec{l}} \tag{5b}$$

is the Fourier transform, on the basis of the lattice vectors $\vec{l}$, of the atomic displacements. Formulas (3)–(5) represent a linear approximation to the cross section in terms of the displacements; in the Al-Li system where the resulting displacements are very small, as we shall see later, this approximation works fairly well.

Hence, a straightforward processing of the experimental intensities gives, via Eqs. (3) and (5), the Fourier transform of the displacement field. From the theoretical side, we proceed to calculate the individual atomic displacements by starting from the ion-electron potential of the Al^{3+} and Li^{+} ions, and compare the resulting $K(\vec{q})$ with the observed data.

B. General formulas for the displacement field

According to the usual method of lattice statics,[3] the lattice distortion is obtained by minimizing the total energy with respect to the individual atomic displacements. For the energy per atom in the dilute solution we can write[8,9]

$$E_{\rm tot} = E_h(\Omega_0,\vec{l}) + c[\Delta E_{\rm per}(\Omega_0,\vec{l}) + \Delta E_{\rm rel}(\vec{u})] + O(c^2) , \tag{6}$$

where E_h is the total energy per atom in the pure *host* metal at an atomic (Wigner-Seitz) volume Ω_0 and $\Delta E_{\rm per}$ is the energy change in a (hypothetical) lattice which is kept to be undistorted, though containing the impurities. The energy of relaxation for one impurity, liberated on removing the hypothetical constraint of geometrical regularity, is

$$\Delta E_{\rm rel} = \sum_{\vec{l},\alpha} f(\vec{l})_\alpha u(\vec{l})_\alpha + \tfrac{1}{2}\sum_{\vec{l},\alpha}\sum_{\vec{l}',\alpha'} (\Phi_{\vec{l}\alpha\vec{l}'\alpha'} + h_{\vec{l}\alpha\vec{l}'\alpha'})u(\vec{l})_\alpha u(\vec{l}')_{\alpha'} + \cdots . \tag{7}$$

We consider, for the moment, the $\vec{u}(\vec{l})$ vectors as variable so that Eq. (7) represents the linear and quadratic terms of the expansion of $(1/c)E_{\rm tot}$ in powers of the atomic displacements, in the presence of one solute atom. Here $f(\vec{l})_\alpha$ and $h_{\vec{l}\alpha\vec{l}'\alpha'}$ determine the displacing force arising from the presence of the impurity and $\Phi_{\vec{l}\alpha\vec{l}'\alpha'}$ is the harmonic "force-constant" matrix of the pure host metal. We limit our discussion to the case when the total "impurity force" acting on the atom at $\vec{l}+\vec{u}(\vec{l})$,

$$-f(\vec{l}+\vec{u}(\vec{l}))_\alpha = -\left(f(\vec{l})_\alpha + \sum_{\vec{l}'\alpha'} h_{\vec{l}\alpha\vec{l}'\alpha'}u(\vec{l}')_{\alpha'}\right) , \tag{8}$$

can be replaced by its value at the ideal lattice site,

$$f(\vec{l})_\alpha + \sum_{\vec{l}'\alpha'} h_{\vec{l}\alpha\vec{l}'\alpha'}u(\vec{l})_{\alpha'} \approx f(\vec{l})_\alpha . \tag{9}$$

This approximation is expected to be valid when the displacements are small; for *Al*Li we find (Sec. IV) that it holds within 5%. By minimizing $E_{\rm tot}$ (i.e., $\Delta E_{\rm rel}$) with respect to $\vec{u}(\vec{l})$ we then get

$$f(\vec{l})_\alpha + \sum_{\vec{l}'\alpha'} \Phi_{\vec{l}\alpha\vec{l}'\alpha'}u(\vec{l}')_{\alpha'} = 0 .$$

We are interested in the strain field due to one single impurity. If this impurity is at site $\vec{L}$, both $\vec{f}$ and $\vec{u}$ depend actually on the relative radius vector $\vec{l}-\vec{L}$. In what follows we choose the impurity site as origin, $\vec{L}=0$. The lattice equilibrium occurs, by Eqs. (7)–(9), at the displacements determined by

$$u(\vec{l})_\alpha = -\sum_{\vec{l}',\alpha'} g_{\vec{l}\alpha\vec{l}'\alpha'} f(\vec{l}')_{\alpha'}, \tag{10}$$

where the matrix $g = \Phi^{-1}$ is the static Green's function of the lattice. By Eq. (5b) we have for $\vec{u}_{\vec{q}}$

$$u(\vec{q})_\alpha = i \sum_\beta g_{\alpha\beta}(\vec{q}) \sum_{\vec{l}} \vec{f}(\vec{l})_\beta \sin(\vec{q}\cdot\vec{l}). \tag{11}$$

Here the Fourier transform of the Green's function is introduced by (BZ denotes Brillouin zone)

$$g_{\vec{l}\alpha\vec{l}'\alpha'} = \frac{\Omega_0}{(2\pi)^3} \int_{BZ} d\vec{q}\, g_{\alpha\beta}(\vec{q}) e^{i\vec{q}\cdot(\vec{l}-\vec{l}')}, \tag{12a}$$

where

$$g_{\alpha\beta}(\vec{q}) = \sum_{\lambda=1,2,3} \frac{e_\alpha(\vec{q},\lambda) e_\beta(\vec{q},\lambda)}{M\omega_{\vec{q}\lambda}^2} \tag{12b}$$

with the traditional notation for polarization vectors $\vec{e}(\vec{q},\lambda)$ and phonon frequencies $\omega_{\vec{q}\lambda}$. The function $\vec{u}(\vec{q})$ is periodic in the reciprocal space and by its definition, Eq. (5b),

$$\vec{u}(\vec{l}) = \frac{\Omega_0}{(2\pi)^3} \int_{BZ} \vec{u}_{\vec{q}} e^{i\vec{q}\cdot\vec{l}}\, d\vec{q}. \tag{13}$$

For a homovalent impurity in a metal, the Fourier transform of the impurity force, needed in Eq. (11), can be obtained in a straightforward fashion in terms of the ion-electron pseudopotentials.[8,9]

If the valence of the host and the impurity atoms are different, the Coulomb interaction also has a contribution to $\vec{f}(\vec{l})$ and, to deal with it, we have to apply an Ewald transformation. As a consequence, we will have the impurity force as a superposition of two terms,

$$\vec{f}(\vec{l}) = \vec{\varphi}(\vec{l}) + \vec{F}(\vec{l}), \tag{14a}$$

where $\vec{\varphi}$ is given by its direct space representation and the other component $\vec{F}$ by its Fourier transform,

$$\vec{F}(\vec{l}) = \frac{i}{N} \sum_{\vec{k}} \vec{k} F(\vec{k}) e^{i\vec{k}\cdot\vec{l}}. \tag{14b}$$

Since $\vec{u}(\vec{q})$ is linear in $\vec{f}$, we have by Eqs. (11)–(14)

$$\vec{u}(\vec{q}) = \vec{u}_1(\vec{q}) + \vec{u}_2(\vec{q}), \tag{15a}$$

with

$$u_1(\vec{q})_\alpha = i \sum_\beta g_{\alpha\beta}(\vec{q}) \sum_{\vec{l}} \varphi(\vec{l})_\beta \sin(\vec{q}\cdot\vec{l}) \tag{15b}$$

and

$$u_2(\vec{q})_\alpha = -i \sum_\beta g_{\alpha\beta}(\vec{q}) \sum_{\vec{G}} (\vec{q}+\vec{G})_\beta F(\vec{q}+\vec{G}). \tag{15c}$$

Hence, in order to determine the strain field $\vec{u}(\vec{q})$ and its scattering amplitude $K(\vec{q})$, we have to calculate the static lattice response function of the host and the distorting force $\vec{f}$ due to the different valency and size of the solute atom. Both these quantities will be obtained in the frame of the perturbed electron-liquid theory, generalizing the treatment for the homovalent solute given previously.[8,9]

According to Eq. (13), the behavior of $\vec{u}(\vec{l})$ far from the solute atom is determined by the form of $\vec{u}(\vec{q})$ near $|\vec{q}| = 0$. By Eqs. (12) and (15) we obtain for the limit $\vec{q} \to 0$

$$u(\vec{q}\to 0)_\alpha \approx -i \sum_\beta \left(\sum_\lambda \frac{e_\alpha(\hat{q},\lambda) e_\beta(\hat{q},\lambda)}{M c_\lambda^2(\hat{q})} \right) \frac{\hat{q}_\beta}{|\vec{q}|} \frac{\Omega_0}{\kappa_h} M_0, \tag{16a}$$

where $c_\lambda(\hat{q})$ is the sound velocity in the direction $\hat{q}$ with polarization λ, κ_h is the compressibility of the host, and for cubic symmetry, we have

$$M_0 = \frac{\kappa_h}{\Omega_0} \lim_{q\to 0} \left\{ F(\vec{q}) + \sum_{\vec{G}\neq 0} \left[F(\vec{q}+\vec{G}) + \tfrac{1}{3} G_\gamma \left(\frac{\partial F(\vec{q}+\vec{G})}{\partial G_\gamma} \right) \right] - \tfrac{1}{3} \sum_{\vec{l}} \varphi(\vec{l})_\gamma l_\gamma \right\}. \tag{16b}$$

M_0 can be called the *asymptotic amplitude* of the displacement field, since it incorporates all effects of the impurity-host interaction as far as the asymptotic strain field is concerned. In fact, for large $|\vec{l}|$ Eq. (16) gives[9]

$$\vec{u}(\vec{l}) \sim \Omega_0 \frac{\vec{A}(\hat{l})}{|\vec{l}|^2} M_0, \tag{17}$$

where the dimensionless vector function $\vec{A}(\hat{l})$, determining the anisotropy of the strain field far from the solute, is derived from the inverse Christoffel matrix of the *pure host*[9] [large parenthesis in Eq. (16a)] and has, therefore, no relation to the properties of the *solute*.

C. Perturbation series for the displacing forces

The perturbation expansion of the total energy for a pure metal[5,6] in terms of the ion-electron potential can easily be generalized[7,8] for the case when impurities are present. Starting from the homogeneous electron liquid, consisting of all valence electrons of the host and impurity atoms and containing the lattice of ions immersed into it, we obtain the total energy per atom, Eq. (6), as

$$E_{tot} = E_0(\bar{n}_0) + E_{es}(Z, Z^*, \vec{R}_{\vec{l}}) + E^{(1)}(Z, Z^*, \Omega_0, \alpha_i, \alpha_i^*) + E^{(2)}(Z, Z^*, \Omega_0, \vec{R}_{\vec{l}}, \alpha_i, \alpha_i^*) + E^{(3)} + E^{(4)} + \cdots, \tag{18}$$

where Z is the charge of the host ion, Z^* is that of the impurity, the average electron density is

$$\bar{n}_0 = \frac{\bar{Z}}{\Omega_0} = \frac{(1-c)Z + cZ^*}{\Omega_0} \tag{19}$$

with an atomic volume Ω_0, E_0 is the energy of the homogeneous electron liquid, and E_{es} stands for the electrostatic energy of the point ions on the background of a uniform negative charge distribution. Further, $E^{(1)}$ is the spatial average of the non-Coulombic part of the mean ion-electron potential,

$$E^{(1)} = \int \left(\bar{v}(\vec{r}) + \frac{\bar{Z}e^2}{|\vec{r}|} \right) \bar{n}_0 d\vec{r} , \tag{20}$$

where

$$\bar{v}(\vec{r}) = (1-c)v(\vec{r}) + cv^*(\vec{r}) .$$

Here $v(\vec{r})$ and $v^*(\vec{r})$ are the "bare" ion-electron potentials for the host and impurity atoms, respectively. These potentials contain some parameters α_i and α_i^* which characterize the host and impurity ions (core, radii, etc.).

For the second-order polarization energy $E^{(2)}$, which represents the contribution from linear screening, we have

$$E^{(2)} = -\tfrac{1}{2} \sum_{\vec{q}} |f_{\vec{q}}|^2 \Omega_0 \frac{P_{\vec{q}}}{\epsilon_{\vec{q}}} , \tag{21}$$

where the dielectric function ϵ is given via the electron polarizability function $P(\vec{q})$ as

$$\epsilon_{\vec{q}} = 1 + \frac{4\pi e^2}{|\vec{q}|^2} P(\vec{q}) .$$

The form of $P(\vec{q})$ depends in a complicated way on the density $\bar{n}_0$ of the electrons that participate in the screening. We do not know this function $P(\vec{q}, n_0)$ exactly, but several approximate forms are known for it. An important property of the exact $P(\vec{q})$ is that, in the limit of small $|\vec{q}|$'s, one has

$$\lim_{\vec{q}=0} P(\vec{q}, n_0) = n_0^2 \left(v_0 \frac{d^2 E_0}{dv_0^2} \right) = n_0^2 \kappa_e , \quad n_0 = \frac{1}{v_0} \tag{22}$$

where κ_e is the static compressibility of the homogeneous electron liquid. Presently, we will use the approximate $P(\vec{q})$ proposed by Toigo and Woodruff[17] and also, for comparison, that given by Geldart and Vosko,[18] and take the Noziéres-Pines form[19] for $E_0(n_0)$. In the one-impurity problem we have[9]

$$f_{\vec{q}} = v_{\vec{q}} \frac{1}{N} \sum_{\vec{l}} e^{-i\vec{q}\cdot\vec{R}_{\vec{l}}} + \frac{1}{N} \Delta v_{\vec{q}} , \tag{23a}$$

with $c = 1/N$ and

$$\Delta v_{\vec{q}} = v_{\vec{q}}^* - v_{\vec{q}} . \tag{23b}$$

The higher-order terms $E^{(3)}$, $E^{(4)}$, etc., are contributions from the *nonlinear screening* by the electrons, and they have more and more complicated analytical forms (see the Appendix). Similarly to the case of pure metals[6] and homovalent alloys,[9] it can be seen that when *the lattice is not distorted*, the contribution from the term $E^{(n)}$ to E_{tot} is of the order $\sim E_F (\bar{v}_{\vec{G}}/E_F)^n$, where $\bar{v}$ stands for v or v^* and E_F is the electronic Fermi energy. Indeed, for the undistorted lattice a factor $(\bar{v}_G)^{n-k}$ appears directly from the first term in (23a) ($k = 0, 1, \ldots, n$), multiplied by integrals over $\vec{q}$ containing $(\Delta v_{\vec{q}})^k$ and this, with the definition of the nth-order electron polarization function,[6] gives the result stated above. Since, however, we will deal specifically with a distorted lattice and thus with derivatives of $E^{(n)}$ with respect to $\vec{u}(\vec{l})$, the convergence in the expansion (18) has to be reconsidered for each particular quantity deduced from E_{tot}, e.g., $\vec{f}(\vec{l})$, Eq. (7).

We proceed now to determine, from Eqs. (18)–(23), the energy contributions according to the grouping in Eq. (6). The electron-liquid energy (per atom) can be written as

$$E_0 = \bar{Z} \epsilon_0(r_s) , \tag{24}$$

where ϵ_0 is the universal function for the energy *per electron* in the interacting electron gas.[19] By Eq. (24) we have, for small c,

$$E_0 = (Z + c\Delta Z) \left[\epsilon_0(r_{s0}) + c \left(\frac{d\epsilon_0}{dr_{s0}} \right) \left(\frac{dr_s}{dc} \right)_{c=0} \right] , \tag{25}$$

where $\Delta Z = Z^* - Z$ and r_{s0} is the radius for an electron in the *host* metal at volume Ω_0, whereas r_s is that in the alloy,

$$\frac{4\pi}{3} r_s^3 = v_0 = \frac{\Omega_0}{\bar{Z}} . \tag{26}$$

We have then by Eq. (19),

$$\left(\frac{dr_s}{dc} \right)_{c=0} = -\frac{r_{s0}}{3} \frac{\Delta Z}{Z} ,$$

leading to

$$E_0 = E_0(\text{host}, \Omega_0) + c \frac{\Delta Z}{Z} \left[E_0(r_{s0}) - \left(\frac{dE_0}{dr_{s0}} \right) \frac{r_{s0}}{3} \right] . \tag{27}$$

For the second term in Eq. (18) we have

$$E_{es} = \frac{1}{2N} \sum_{\vec{l} \neq \vec{l}'} \frac{Z_l Z_{l'} e^2}{|\vec{R}_{\vec{l}} - \vec{R}_{\vec{l}'}|} - \tfrac{1}{2} Z e^2 \int \frac{n_0 d\vec{r}}{|\vec{r}|} ,$$

which can be transformed by the usual Ewald method to the form

$$E_{es} = E_{es}(\text{host}, \Omega_0) + cZ\Delta Z e^2 \left\{ \sum_{\vec{l}=0} \frac{1}{|\vec{R}_{\vec{l}}|} \operatorname{erfc}(\eta |\vec{R}_{\vec{l}}|) - \frac{2\eta}{\sqrt{\pi}} + \frac{2\pi}{\Omega_0} \sum_{\vec{k} \neq 0} \left(\frac{1}{|\vec{k}|^2} e^{-|\vec{k}|^2/4\eta^2} \frac{1}{N} \sum_{\vec{l}} 2\cos(\vec{k}\cdot\vec{R}_{\vec{l}}) \right) - \frac{\pi}{\Omega_0 \eta^2} \right\} \tag{28}$$

for one impurity at the origin. Here $\mathrm{erfc}(x)$ is the complementary error function, and the arbitrary parameter η is chosen so as to give the most convenient convergence of the series in Eq. (28). When site symmetry in the pure host includes inversion, we can write this equation as

$$E_{es}=\left(1+2\frac{\Delta Z}{Z}c\right)\left(-\frac{Z^2e^2}{2R_a}\gamma\right)+\frac{1}{N}\sum_{\vec{l}}[\vec{\Phi}_{\vec{l}}+\vec{F}_M(\vec{l})]\vec{u}(\vec{l})+\frac{1}{2N}\sum_{\vec{l}\alpha}\sum_{\vec{l}'\alpha'}\Phi^M_{\vec{l}\alpha\vec{l}'\alpha'}u(\vec{l})_\alpha u(\vec{l}')_{\alpha'}+\cdots, \tag{29}$$

where R_a is the radius of an atomic sphere in the alloy, γ is the usual Madelung constant, and the coefficients $\Phi^M_{\vec{l}\alpha\vec{l}'\alpha'}$ are the contributions of the electrostatic forces to the force-constant matrix of the pure host. The Coulomb contribution to the displacing forces has the form

$$\vec{\varphi}(\vec{l})=Z\Delta Ze^2\frac{\partial}{\partial\vec{r}}\left(\frac{1}{|\vec{r}|}\,\mathrm{erfc}(\eta|\vec{r}|)\right)_{\vec{r}=\vec{l}} \tag{30a}$$

and

$$\vec{F}_M(\vec{l})=Z\Delta Ze^2\frac{i}{N}\sum_{\vec{k}}\left(\vec{k}\frac{4\pi}{\Omega_0|\vec{k}|^2}e^{-|\vec{k}|^2/4\eta^2}\right)e^{i\vec{k}\cdot\vec{l}}. \tag{30b}$$

For the next term in Eq. (18) we have

$$E^{(1)}=\frac{\bar{Z}\bar{\beta}}{\Omega_0}=\frac{\bar{Z}[\beta+c(\beta^*-\beta)]}{\Omega_0}, \tag{31a}$$

where

$$\beta=\int\left(v+\frac{Ze^2}{|\vec{r}|}\right)d\vec{r},\quad \beta^*=\int\left(v^*+\frac{Z^*e^2}{|\vec{r}|}\right)d\vec{r}, \tag{31b}$$

so that, writing $\beta^*-\beta=\Delta\beta$, one has for the average non-Coulombic potential energy

$$E^{(1)}=E^{(1)}(\mathrm{host},\Omega_0)+c\Delta E^{(1)}$$

with (32)

$$\Delta E^{(1)}=\frac{Z\Delta\beta}{\Omega_0}+\frac{\beta\Delta Z}{\Omega_0}.$$

Similarly, the contribution from linear screening to the polarization energy has the form, via Eqs. (21) and (23),

$$E^{(2)}=E^{(2)}(\mathrm{host},\Omega_0)+c\Delta E^{(2)}, \tag{33}$$

where

$$E^{(2)}(\mathrm{host},\Omega_0)=-\tfrac{1}{2}\sum_{\vec{G}}|v_{\vec{G}}|^2\Omega_0\frac{P(\vec{G},n_0)}{\epsilon(\vec{G},n_0)}+\frac{1}{2N}\sum_{\vec{l}\alpha}\sum_{\vec{l}'\alpha'}\Phi^P_{\vec{l}\alpha\vec{l}'\alpha}u(\vec{l})u(\vec{l})_{\alpha'}. \tag{34}$$

Here $\vec{G}$ is a vector of the reciprocal lattice and Φ^P stands for the linear screening contribution to the dynamical matrix. We write the argument n_0 in P and ϵ explicitly to emphasize that $E^{(2)}$(host) is calculated at an electron density Z/Ω_0. Terms linear in $\vec{u}$ do not arise in Eq. (34) when site symmetry includes inversion. For the second term in Eq. (33) we have

$$\Delta E^{(2)}=-\sum_{\vec{G}}v_{\vec{G}}\Delta v_{\vec{G}}\Omega_0\frac{P_{\vec{G}}}{\epsilon_{\vec{G}}}-\frac{1}{2N}\sum_{\vec{q}}|\Delta v_{\vec{q}}|^2\Omega_0\frac{P_{\vec{q}}}{\epsilon_{\vec{q}}}+\Delta Z\sum_{\vec{G}}-\tfrac{1}{2}|v_{\vec{G}}|^2\frac{\partial}{\partial n_0}\left(\frac{P_{\vec{G}}}{\epsilon_{\vec{G}}}\right)+\frac{1}{N}\sum_{\vec{l}}F^{(2)}(\vec{l})_\alpha u(\vec{l})_\alpha. \tag{35}$$

Here the first two terms are the same as for a homovalent impurity.[9] In the heterovalent case, however, the density of the responding electrons also varies with c, and the third term in Eq. (35) takes this variation into account, being the derivative of the first term in Eq. (34). The linear screening contribution to the impurity forces is obtained as

$$\vec{F}^{(2)}(\vec{l})=\frac{i}{N}\sum_{\vec{k}}\vec{k}\left(-v_{\vec{k}}\Delta v_{\vec{k}}\Omega_0\frac{P_{\vec{k}}}{\epsilon_{\vec{k}}}\right)e^{i\vec{k}\cdot\vec{l}}. \tag{36}$$

By using Eqs. (25)–(29) and (32)–(35), we can now rearrange the perturbation series Eq. (18) to the form required by the lattice statics method. For the "undistorted part" of the energy we have

$$\Delta E_{\mathrm{per}}=\Delta Z\left[\epsilon_0(r_{s0})-\left(\frac{d\epsilon_0}{dr_{s0}}\right)\frac{r_{s0}}{3}\right]+2\frac{\Delta Z}{Z}\left(-\frac{Z^2e^2}{2R_a}\gamma\right)+\left(\frac{Z\Delta\beta}{\Omega_0}+\frac{\beta\Delta Z}{\Omega_0}\right)+\Delta Z\left[-\tfrac{1}{2}\sum_{\vec{G}}|v_{\vec{G}}|^2\frac{\partial}{\partial n_0}\left(\frac{P_{\vec{G}}}{\epsilon_{\vec{G}}}\right)\right]-\sum_{\vec{G}}v_{\vec{G}}\Delta v_{\vec{G}}\Omega_0\frac{P_{\vec{G}}}{\epsilon_{\vec{G}}}-\frac{1}{2N}\sum_{\vec{q}}|\Delta v_{\vec{q}}|^2\Omega_0\frac{P_{\vec{q}}}{\epsilon_{\vec{q}}}. \tag{37}$$

The three terms in Eq. (37) which do not contain the multiplying factor ΔZ represent the expression for ΔE_{per} in the case of a homovalent impurity.[8,9]

Since ΔE_{per} refers specifically to a lattice which is not distorted, stopping at, for example the linear screening term $E^{(2)}$ in (18) implies for this quantity an accuracy of $\sim(\tilde{v}_{\vec{G}}/E_F)^2$, as discussed above. For the impurity force we obtain, by Eqs. (30) and (36),

$$\vec{\varphi}(\vec{l})=Z\Delta Ze^2\frac{\partial}{\partial\vec{r}}\left(\frac{1}{|\vec{r}|}\mathrm{erfc}(\eta|\vec{r}|)\right)_{\vec{r}=\vec{l}} \tag{38}$$

and

$$F(\vec{k})=Z\Delta Ze^2\frac{4\pi}{\Omega_0|\vec{k}|^2}e^{-|\vec{k}|^2/4\eta^2}-v_{\vec{k}}\Delta v_{\vec{k}}\Omega_0\frac{P_{\vec{k}}}{\epsilon_{\vec{k}}}+F^{(3)}+F^{(4)}+\cdots. \tag{39}$$

We will see in the next paragraph that both $F^{(3)}$ and $F^{(4)}$ are to be retained together with the linear screening term, if we calculate $\vec{u}(\vec{q})$ [and $K(\vec{q})$] at *small* $|\vec{q}|$ values. The explicit forms for $F^{(3)}$ and $F^{(4)}$ are given in the Appendix.

The individual atomic displacement can now be calculated according to Eqs. (10), (12), (13), and (39) provided we know the ion-electron potentials $v(\vec{q})$ and $v^*(\vec{q})$. In the present work local Heine-Abarenkov model potentials will be used, with two parameters each, since for both pure Al and pure Li such a description has been seen[6,8,20,21] to work reasonably well. First, however, we analyze the behavior of $F(\vec{k})$ for $|\vec{k}| \to 0$.

D. The long-wave limit of $F(\vec{k})$ and the volume change

We consider now the convergence of the expansion Eq. (39) for $F(\vec{k})$. To obtain $F^{(n)}$ we have to differentiate the perturbation series Eq. (18) for E_{tot} with respect to the displacements. The same argument as that used in the preceding paragraph for ΔE_{per} shows that for a *general* wave vector $\vec{q} \lesssim |\vec{G}|$ a factor of the order $\sim(\tilde{v}_{\vec{G}}/E_F)^n$ appears also in $F^{(n)}$. However, this is *not* so for $|\vec{q}| \ll |\vec{G}|$, and we get the clearest demonstration of this by considering the limiting value at $|\vec{q}| = 0$. To arrive at $\vec{u}(\vec{q} \to 0)$ we need to calculate M_0 [Eqs. (16a) and (16b)] by using the series equation (39) for $F(\vec{k})$. From the expressions (A2) and (A3) for $F^{(3)}$ and $F^{(4)}$ we find immediately that the following terms in M_0 are of the same smallness as $F^{(2)}(\vec{G})$,

$$F^{(3)}(0) = -n_0 \frac{\partial}{\partial n_0}\left(\sum_{\vec{G}} v_{\vec{G}} \Delta v_{\vec{G}} \Omega_0 \frac{P_{\vec{G}}}{\epsilon_{\vec{G}}} + \frac{1}{2N}\sum_{\vec{q}} |\Delta v_{\vec{q}}|^2 \Omega_0 \frac{P_{\vec{q}}}{\epsilon_{\vec{q}}}\right), \tag{40a}$$

$$\lim_{\vec{q}=0} F^{(3)}(\vec{q}+\vec{G}) = \left(\frac{\Delta v}{\epsilon}\right)_{\vec{q}\to 0} \Omega_0 P_0 |v_{\vec{G}}|^2 \frac{\partial}{\partial n_0}\left(\frac{P_{\vec{G}}}{\epsilon_{\vec{G}}}\right) + \cdots, \tag{40b}$$

$$\lim_{\vec{q}=0} \tfrac{1}{3} G_\gamma \frac{\partial}{\partial G_\gamma}[F^{(3)}(\vec{q}+\vec{G})] = \left(\frac{\Delta v}{\epsilon}\right)_{\vec{q}\to 0} \Omega_0 P_0 \tfrac{1}{3} G_\gamma \frac{\partial}{\partial G_\gamma}\left[\tfrac{1}{2}|v_{\vec{G}}|^2 \frac{\partial}{\partial n_0}\left(\frac{P_{\vec{G}}}{\epsilon_{\vec{G}}}\right)\right] + \cdots, \tag{40c}$$

and

$$\lim_{\vec{q}=0} F^{(4)}(\vec{q}) = -\left(\frac{\Delta v}{\epsilon}\right)_{\vec{q}\to 0} \Omega_0 P_0 \sum_{\vec{G}} -\tfrac{1}{2}|v_{\vec{G}}|^2 n_0 \frac{\partial^2}{\partial n_0^2}\left(\frac{P_{\vec{G}}}{\epsilon_{\vec{G}}}\right) + \cdots, \tag{40d}$$

In Eq. (40b)–(40d) lower order terms are left and in Eq. (40a) and (40d) $P_0(v/\epsilon)_{\vec{q}\to 0} = -n_0$ was used.[9] Further, we have

$$\Omega_0 P_0 \lim_{q=0}\left(\frac{\Delta v_{\vec{q}}}{\epsilon_{\vec{q}}}\right) = \Omega_0 P_0 \lim_{\vec{q}=0} \frac{q^2}{4\pi e^2}\frac{1}{P_{\vec{q}}}\left(-\frac{4\pi \Delta Z e^2}{\Omega_0 |\vec{q}|^2} + \frac{\Delta\beta}{\Omega_0}\right) = -\Delta Z, \tag{41}$$

hence, these *formally* third- and fourth-order expressions, at nearly zero argument, are indeed of the order $\sim E_F(\tilde{v}_{\vec{G}}/E_F)^2$. Expression (40a) of $F^{(3)}(0)$, appearing also for *homovalent* alloys, has already been found previously[9]; the three other terms in Eqs. (40b)–(40d) are new results. We see that each of these four contributions has to be included in the calculation of the *asymptotic* amplitude of the displacement field, Eq. (16), whereas only $F^{(2)}(\vec{q})$ is important for a general $|\vec{q}| \lesssim |\vec{G}|$. This means that, on applying the lattice statics method, Eqs. (11) and (12), to calculate $\vec{u}(\vec{q})$, the terms $F^{(3)}$ and $F^{(4)}$ become *progressively* more and more important when going toward $\vec{q} = 0$, and neglecting them leads, in particular, to a *wrong limit at* $\vec{q} = 0$.

The result (40) and (41) also shows how the contribution of $F^{(3)}(\vec{q})$ and $F^{(4)}(\vec{q})$ to M_0 can be calculated *without* the explicit use of the complicated nonlinear screening functions $\Lambda^{(n)}$ (see the Appendix) at the single point $\vec{q} = 0$. To clarify the signification of this result, we refer to the well known fact that $\vec{u}(\vec{q} \to 0)$ and the volume change per solute atom $\Delta\Omega_0$ are interrelated.[3,22] We can write this relation as

$$\frac{\Delta\Omega_0}{\Omega_0} \equiv \frac{1}{\Omega_0}\left(\frac{d\Omega_0}{dc}\right)_{c=0} = M_0, \tag{42}$$

where M_0 determines, according to Eqs. (16) and (17), the long-range displacement field. This equation follows directly from the general result[22] which, for cubic crystals, tells us that

$$\Delta\Omega_0 = -\kappa_h \tfrac{1}{3} \sum_{\vec{l},\alpha} f(\vec{l}+\vec{u}(\vec{l}))_\alpha l_\alpha. \tag{43}$$

Indeed, by substituting Eq. (14) for the force $\vec{f}$ and neglecting $\vec{u}$ in the argument, we arrive from Eq. (43) at Eq. (42) with M_0 defined in Eq. (16b).

On the other hand, the equilibrium volume and thus $\Delta\Omega_0$ can also be obtained by minimizing the total energy [Eq. (6)] with respect to Ω_0 at a given c. This gives, by Eq. (6),

$$\frac{\Delta\Omega_0}{\Omega_0} = -\kappa_h\left(\frac{d\Delta E_{per}}{d\Omega_0} + \frac{d\Delta E_{rel}}{d\Omega_0}\right) - \kappa_h\left(\frac{d\Delta E_{per}}{d\Omega_0}\right). \tag{44}$$

For very small displacements we can neglect the second term within the first set of large parentheses of this equation, within the same accuracy[23] as $\vec{f}(\vec{l}+\vec{u}) \approx \vec{f}(\vec{l})$ in Eqs. (9) and (43). We will

see that for AlLi this approximation is extremely good. The two ways of calculating $\Delta\Omega_0$, Eqs. (42) and (44), must lead to the same result; thus we have to check the validity of the identity

$$-\frac{d\Delta E_{\rm per}}{d\Omega_0}=\frac{M_0}{\kappa_h}. \tag{45}$$

Two remarks have to be made at this point. First, the derivation on the left-hand side has to be performed according to the rule[6]

$$\frac{d}{d\Omega_0}=\left(\frac{\partial}{\partial\Omega_0}\right)_{\vec{G},n_0}-\frac{1}{3\Omega_0}G_\alpha\left(\frac{\partial}{\partial G_\alpha}\right)_{\Omega_0,n_0}-\frac{n_0}{\Omega_0}\left(\frac{\partial}{\partial n_0}\right)_{\Omega_0,\vec{G}}, \tag{46}$$

since $\Delta E_{\rm per}$, Eq. (37), depends on the volume explicitly via $\vec{G}$ and also through n_0 appearing in the screening function. With this, by comparing the two sides of Eq. (45) we find that the terms corresponding to the derivatives $\partial/\partial n_0$ and $\partial^2/\partial n_0^2$, arising from the volume derivation of $\Delta E_{\rm per}$, can be identified on the right-hand side as precisely the terms $F^{(3)}(0)$, etc., of Eqs. (40a)–(40d) contributing to M_0. Then, by a term-by-term comparison, Eq. (45) reduces to

$$-\Delta Z\Omega_0\frac{d}{d\Omega_0}\left[\epsilon(r_{s0})-\frac{r_{s0}}{3}\left(\frac{d\epsilon_0}{dr_{s0}}\right)\right]=\frac{Z\Delta Z}{\Omega_0 P_0} \tag{47}$$

as the condition for the theory to be consistent. We can recognize, however, that this equation is not "new" but just another form of the compressibility limit Eq. (22). Indeed, one has

$$-\Omega_0\frac{d}{d\Omega_0}\left[\epsilon(r_{s0})-\frac{r_{s0}}{3}\left(\frac{d\epsilon_0}{dr_{s0}}\right)\right]=v_0^2\frac{d^2\epsilon_0}{dv_0^2}=\frac{1}{n_0\kappa_e}.$$

The presence of significant nonlinear screening contributions and the necessity to have the accurate value for $P(\vec{q}\to 0)$ reminds one of the problem of the calculation of compressibility for pure simple metals.[6] The situation is similar in the two cases: Nonlinear screening terms of third and fourth order become large at long wavelength, of the same order as the "main" linear screening contribution, both for the longitudinal sound velocity of the pure metal and for the distorting force in the dilute alloy. The analogy is, however, not complete as shown immediately by the important differences in the result for homovalent and heterovalent solutes: The fourth-order term $F^{(4)}(0)$ does not appear at all for $Z^*=Z$. The particularity of the alloy problem is that the derivatives $\partial/\partial n_0$ and $\partial^2/\partial n_0^2$ in the "impurity pressure," Eq. (45), have a double origin. First, for $Z^*\neq Z$ the variation of the electronic density with the *concentration* generates a term in the energy [Eq. (35)] which contains the density derivative of the dielectric function. Then, in obtaining the pressure from $\Delta E_{\rm per}$ we use Eq. (46), and the operation $\partial/\partial n_0$ appears again. This clarifies the essential difference between $Z^*\neq Z$ and $Z^*=Z$: In the homovalent alloy the density of the responding homogeneous electron liquid does not vary with the concentration; therefore the corresponding derivative is lacking. Physically, the additional new terms for $Z^*\neq Z$ show the increased role of nonlinear screening for a heterovalent solute, which is quite understandable, since the perturbation, realized by the difference Δv in the ionic potentials, is much more important for $\Delta Z\neq 0$ and survives even in the Coulombic range. Similarly, Eq. (46) shows that the correct limit $P(\vec{q}=0)$ is as crucial in the calculation of the volume change as it is in calculating the pure metal compressibility,[6] but we arrive at this condition only for $\Delta Z\neq 0$.

The role of the different terms arising from the different contributions to $\Delta E_{\rm per}$ [Eq. (37)] will be discussed in the specific example of AlLi in Sec. IV B. We mention that one aspect of the problem, the twofold variation of the electronic density in determining the volume change due to a nonhomovalent defect, has already been noticed[20,21] in the context of the formation volume of a vacancy.

IV. NUMERICAL RESULTS

A. Ion-electron potentials for solute and solvent

For both Al^{3+} and Li^+ we describe the bare ion-electron interactions by a model potential of the local Heine-Abarenkov type[5,6]

$$v(\vec{r})=\begin{cases}-\dfrac{Ze^2}{|\vec{r}|}, & r\geq R_c\\[2ex] -\lambda\dfrac{Ze^2}{R_c}, & r<R_c\end{cases} \tag{48}$$

which gives, when Fourier-transformed,

$$v(q)=-\frac{4\pi Ze^2}{\Omega_0 q^2}\left((1-\lambda)\cos(qR_c)+\lambda\frac{\sin(qR_c)}{qR_c}\right), \tag{49}$$

so that, e.g., the parameter β defined in Eq. (31b) is obtained as

$$\beta=4\pi Ze^2R_c^2\left(\frac{1}{2}-\frac{\lambda}{3}\right).$$

According to the original prescription,[5,6] $v(q)$ in Eq. (49) was multiplied by the cutoff factor $\exp[-\zeta(q/2k_F)^4]$; the value of ζ was fixed as[6] 0.03 (Li) and 0.15 (Al).

The parameters R_c and λ can be determined in both cases by requiring that the lattice constant *and* the elastic constant c_{44} coincide, for the *pure* solvent and solute metals, with their observed

values. For the case of the alkali metals this method of fixing the model potential parameters can already be considered as standard,[6,8,20,21,24,25] and tabulated values, for different screening functions, are available[8,24,25] for Li. For aluminium, however, we may have somewhat different choices, substituting the requirement of an *exact* reproduction of c_{44} by that of the bulk modulus[20] or of an optimum overall fit to the phonon spectrum.[6] This is so since, in the case of aluminium, fitting of c_{44} does not ensure an optimum reproduction of *all* the elastic constants and the phonon dispersion curves. In Fig. 3 the curve indicates the interrelated values of R_c and λ for which the calculated lattice constant agrees with the experimental value. The points where c_{44} equals its experimental value are indicated in the plot. We see, first, that the conditions of reproducing the lattice spacing and c_{44} do not determine R_c and λ unambiguously: We have *two* pairs of parameters satisfying these two conditions.

At this point we notice that R_c in Eq. (48) has the physical meaning of a radius of the Al^{3+} ion, outside which the ion-electron interaction is merely Coulombic attraction. Hence, R_c may not differ very much from the Pauling ionic radius, $R_P = 0.945$ a.u. for Al^{3+}; the Ashcroft empty-core radius ($\lambda = 0$) was, e.g., found[26] to be $R_A = 1.12$ a.u. We see that one of the two R_c's found by our method can well have the meaning of a radius separating Coulombic and non-Coulombic ranges of the potential, but the root $R_c = 2.45$ a.u. is too large to be so interpreted. A prototype of such a "large-R_c" potential, with R_c outside the range of a reasonable ionic radius, with $\lambda = 1$, has been studied recently[27] and found to reproduce fairly well trends in elastic moduli of simple metals, provided the first zero of $v(q)$ is chosen near to the Heine-Abarenkov value. Still, we want to attach physical significance to R_c as a core radius, and consider only the $R_c \cong 1$ a.u. solution as physical. The results obtained by the "too large" R_c's (for Al as well as for Li) will only briefly be mentioned.

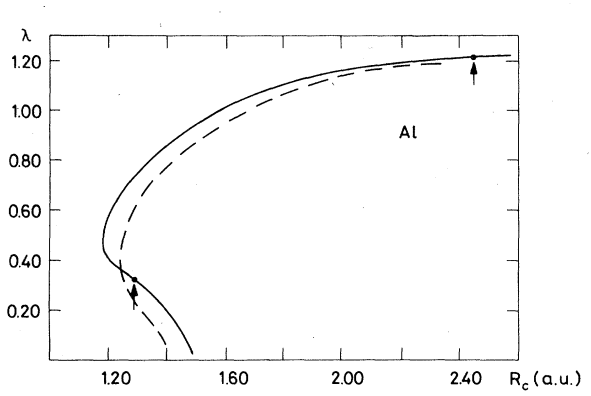

FIG. 3. Model potential parameters (R_c, λ) which ensure zero pressure at the observed lattice spacing in Al. The solid line corresponds to the TW approximation (Ref. 17) for screening, while the dotted line corresponds to the GV dielectric function (Ref. 18). The arrows indicate the parameter values which, in addition, reproduce the shear modulus c_{44}.

In Table I, the first two columns contain the experimental input data by which the parameters of our model potentials are determined, as listed in the next two columns. The potentials so obtained have been checked by calculating the bulk modulus, the other shear modulus, and the total binding energy for both metals, and comparison with the observed data is shown in the next columns of Table I. For lithium the parameters are the same as used already in previous work,[24,25] giving remarkably good agreement for the elastic constants and the phonon spectrum in general, though with some overshoot of the binding energy. The Al row corresponds to the potential determined by the same method as used for lithium, whereas the row Al* refers to the potential obtained by fitting R_a and yielding the best overall fit for the phonons; the numbers in this row are near to those given in the literature.[6,20] In the row Al** the potential with "nonphysical" R_c is presented.

Having thus found the bare model potentials which describe reasonably well both the solvent and the solute metals *before* alloying, we proceed to calculate the expected properties of the *dilute alloy*.

B. Volume change and lattice strain in the alloy

Among the data for the partial volume change in dilute *Al*Li solid solutions we find two experimental results.[1,2] Both agree in that aluminium *contracts* on dissolving lithium atoms, and the relative changes in lattice constant per dissolved Li atom are, by a quadratic interpolation, $(1/a) \times (da/dc)_{c=0} = -0.016 \pm 0.001$, according to Ref. 1, and -0.008 ± 0.001, according to Ref. 2, where a is the lattice constant for pure aluminium. However small, such a contraction is unexpected, insofar as any kind of interpolation between the Wigner-Seitz radii of pure Al and Li necessarily leads to an *increase* in the lattice spacing, since R_a for lithium is appreciably larger, by 9%, than that for aluminium (see Table I). To explain these experimental results, some qualitative arguments have been put forward.[1] It was pointed out that the cohesive forces, active in metallic lithium and determining its lattice spacing, are almost negligibly small as compared to the same forces in aluminium metal, due to the 3 times larger ionic charge and to the correspondingly larger

TABLE I. Potential parameters for pure Li and Al, Eq. (48). The values for R_c and λ have been determined by reproducing R_a and c_{44} for each metal, except for the rows Al* and Al** where agreement with R_a and an optimum overall fit for the phonon dispersion curves was required. In the rows Li, Al, and Al* results for both the Toigo-Woodruff (TW, Ref. 17) and Geldart-Vosko (GV, Ref. 18) screening approximations are shown. The same (λ, R_c) values for Li have been published previously (Refs. 24 and 25). The binding energy E_{bind} is the sum of the ionization energy and the heat of sublimation at 0 K, given in Ry. The unit for the elastic constants is 10^9 dyn/cm^2.

	Experimental input data		Potential parameters			Calculated properties for solvent and solute		
	R_a (a.u.)	c_{44}		R_c (a.u.)	λ	B	$(c_{11}-c_{12})/2$	E_{bind}
Li	3.237[a]	113[b]	TW	1.534	0.371	135	10.6	−0.551
			GV	1.512	0.334	135	10.6	−0.551
						expt. 130[b]	11.2[b]	−0.518[b,c]
Al	2.978[a]	316[d]	TW	1.247	0.350	571	216	−4.298
			GV	1.273	0.542	651	122	−4.465
						expt. 794[d]	262[d]	−4.159[c]
Al*	2.978[a]	395[d]	TW	1.2685	0.332	618	260	−4.242
		423	GV	1.247	0.361	674	192	−4.307
		expt. 316[d]				expt. 794[d]	262[d]	−4.159[c]
Al**	2.978[a]	426	TW	2.451	1.211	654	261	−4.306
		expt. 316[d]				expt. 794[d]	262[d]	−4.159[c]

[a] *Landolt-Börnstein: Numerical Data and Functional Relationships*, edited by K.-H. Hellwege and A. M. Hellwege (Springer, Berlin, 1971), Group III, Vol. 6.

[b] Reference 25.

[c] K. A. Gschneidner, in *Solid State Physics*, edited by F. Seitz and D. Turnbull (Academic, New York, 1964), Vol. 16.

[d] G. N. Kamm and G. A. Alers, J. Appl. Phys. 35, 32 (1964).

electronic density in Al. The argument suggests that the value of the Wigner-Seitz radius in *pure* metallic lithium has, thereby, no significance at all in determining the volume in the dilute *solution*, which contains a few Li atoms dissolved in the Al "block." In the same spirit, a more refined version[28] of Vegard's law takes into account the difference in compressibility for solvent and solute, and predicts for *Al*Li only one third of the expansion expected by the simple volume interpolation. This would still be large and positive, however.

To investigate the problem quantitatively, we have calculated the different contributions to the "impurity pressure,"

$$\Delta p \equiv -\frac{d\Delta E_{\text{per}}}{d\Omega_0} = \Delta p_{\text{EL}} + \Delta p_{\text{Mad}} + \Delta p_{\text{av}} + \Delta p_{\text{BS}} + \Delta p_c + \Delta p_i \,, \tag{50}$$

and show the results in Table II. The six pressure contributions in Eq. (50) arise, term by term, from the corresponding expressions in Eq. (37). We can speak, according to this classification, of the "partial" pressures associated with the energy of the electron liquid (EL) the electrostatic (Madelung) energy, the energy of the average non-Coulombic part of the potential, the second-order "band-structure" (BS) energy, the coherent and the incoherent alloying energies, respectively [see Eq. (37).] It is the sum of these partial pressures, according to Eqs. (50) and (37), which "forces" the solvent to contract or expand, depending on its sign, and the relative volume change is given by scaling Δp by the bulk modulus of the host $1/\kappa_h$. In Table II one sees that changing a $Z = 3$ point ion into one with $Z^* = 1$ would, other effects being absent, *increase* the volume considerably, Δp_{Mad} is large and positive. This is easy to understand, since the *decrease* in the electrostatic binding energy, associated with $Z^* < Z$, is the smaller the lattice spacing is larger. About two-thirds of this positive pressure is, however, canceled out already by the large, negative Δp_{av}, showing that the electrostatic effect is largely reduced by the finite dimensions of the cores, inside which there is no Coulomb attraction [see Eqs. (20) and (48)]. The remaining one-third of the positive pressure is, nevertheless,

TABLE II. Contributions to the internal pressure per solute atom in *Al*Li, leading to the limiting partial volume change $\Delta\Omega_0$ [Eqs. (50) and (37)]. The pressure unit is kbar; the notation Al* refers to the model parameters given in Table I. The values in square brackets are those obtained by neglecting the variation of the electronic density in the screening function $P(\vec{q})$; their use leads to the pressures $[\Delta p]$ of the 8th column. The column $[\Delta p]_F$ is the result by calculating $\vec{u}(\vec{q}\to 0)$, according to Eqs. (16a) and (16b) but neglecting nonlinear screening terms $F^{(3)}(\vec{k})$ and $F^{(4)}(\vec{k})$. One has $[\Delta p]=[\Delta p]_F$ if Eq. (22) for $P(\vec{q})$ is exactly satisfied.

	Δp_{EL}	Δp_{Mad}	Δp_{av}	Δp_{BS}	Δp_c	Δp_i	Δp	$[\Delta p]$	$[\Delta p]_F$	$100\frac{\Delta\Omega_0}{\Omega_0}$
Al* TW			−2028	14	−106	−108	−13			−1.6
				[0]	[−193]	[0]		−6	−33	
	−976	3191								
Al* GV			−1863	−15	−255	−129	−47			−5.9
				[0]	[−330]	[0]		+22	+22	
Experiment										-4.8 ± 0.5[a]
										-2.5 ± 0.5[b]

[a] Reference 1.
[b] Reference 2.

still of the order of ~1 Mbar, and this, in turn, is almost completely neutralized by the negative contribution Δp_{EL} of the electron liquid energy. This is so because the electron liquid in aluminium is in a strongly compressed state ($r_s=2.07$), and each Li atom is "welcome" as it reduces the conduction-electron density. After adding these three "big" contributions, we have already a relatively small pressure of ~200 kbar, which is at the end, slightly overbalanced by the three small, negative pressures Δp_{BS}, Δp_c, Δp_i, containing quadratic expressions of the ion-electron potentials.

The calculated values also show the importance of the pressure associated with the variation of the electronic density in $P(\vec{q},n_0)$. In fact, due to the large cancellation and the resultingly small value of Δp, these contributions are far from being negligible. From the point of view of the calculation of the impurity force, and thus of $K(\vec{q})$ and $\vec{u}(\vec{q})$, this means that at small $\vec{q}$'s the terms $F^{(3)}$ and $F^{(4)}$ are *also numerically* important, contributing, for example, 14, 87, and −108 kbar, to be compared with the result of −13 kbar (see Table II).

As far as the approximations for the screening function are concerned, we see that both the Geldart-Vosko (GV) and Toigo-Woodruff (TW) results for $\Delta\Omega_0$ are reasonable. We find, *independently* of the approximation for screening, *anomalously small* values for $\Delta\Omega_0/\Omega_0$ (−1.6% and −5.9%), which are in the order of the observed values. In turn, an estimation based on the interpolation of the volumes of solvent and solute (Vegard's law) would suggest $\Delta\Omega_0/\Omega_0\approx+25\%$. We note that, although the TW polarization function at a general $|\vec{q}|$ is superior to the GV formula, this is not so at $\vec{q}=0$, where Eq. (22) is satisfied *exactly* by the GV function whereas only within a certain numerical accuracy for the TW function (~4% in the present case). This is why, using the values in square brackets in the first row of Table II, the result (8th column) is not equal to that found by the "linear screening asymptotics" of $\vec{u}(\vec{q}\to 0)$ (9th column) for the TW function. This small numerical discrepancy for the TW screening approximation is, however, not important, since the linear screening value for $\vec{u}(\vec{q}\to 0)$ is, anyway, irrelevant as discussed above. The validity of the approximation Eq. (44) which consists in neglecting the volume derivative of ΔE_{rel} was also checked, and a value $\Delta p_{rel}\sim 2\times10^{-3}$ kbar was obtained. In Figs. 4 and 5 the scattering cross sections per solute atom, Eq. (3), are plotted for the symmetry directions [110], [100], and [111]. First, the experimental results reproduce the Laue scattering, Eq. (2), very well. The values for $\vec{q}\to 0$ are calculated via Eqs. (5), (16a), (45), and (50) with the result

$$\lim_{\vec{q}=0} K(\vec{q}) = -\frac{\Omega_0\Delta p}{Mc_t^2(\vec{q})} = -\frac{B}{\tilde{c}}\frac{\Delta\Omega_0}{\Omega_0}\ , \qquad (51)$$

where $\tilde{c}$ is c_{11}, $\frac{1}{2}(c_{11}+c_{12}+2c_{44})$, and $\frac{1}{3}(c_{11}+2c_{12}+4c_{44})$ for the [110], [100], and [111] directions, respectively, so that with the experimental values of c_{ik} (Table I) we arrive at 0.66, 0.69, and 0.65 for $B/\tilde{c}$. The values of $K(\vec{q}\to 0)$ and $(d\sigma/d\vec{\Omega})$ $(\vec{q}\to 0)$ for the [110] direction are given in the last row of Table III, using $B/\tilde{c}=0.66$ and the *observed* values for $\Delta\Omega_0/\Omega_0$. We notice that in the three symmetry directions the difference in $(d\sigma/d\vec{\Omega})$ $(\vec{q}=0)$ is small, maximum 0.3%, and not observable by the

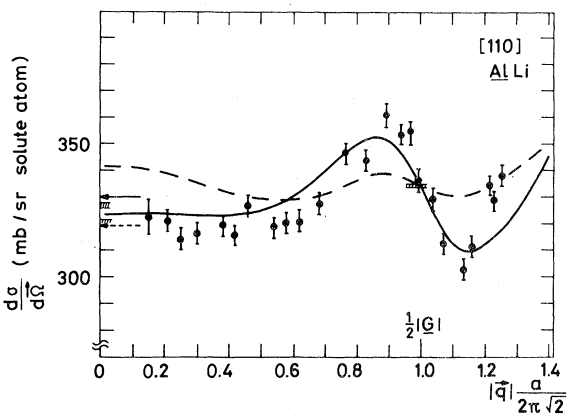

FIG. 4. Diffuse elastic neutron cross section of scattering by the lattice distortion in *Al* Li solid solution, Eq. (3). The theoretical curves are calculated by the lattice statics method, in linear screening approximation; the difference in solid and dashed lines is due to the different choice of the electronic polarization function (TW and GV screening approximations, respectively). The potential parameters are those in the Al* row of Table I. If the contributions of nonlinear screening into the impurity force are taken into account, the curves should arrive at the corresponding limiting values indicated by the arrows at $\vec{q}=0$ (Table III). The hatched strip at $|\vec{q}| = \frac{1}{2}|\vec{G}|$ is the expected value of $d\sigma/d\vec{\Omega}$ with $K(\vec{q})=0$ (Laue scattering), and the strips at $\vec{q}=0$ are calculated by using the observed volume change, according to the independent experiments (Ref. 1 and 2).

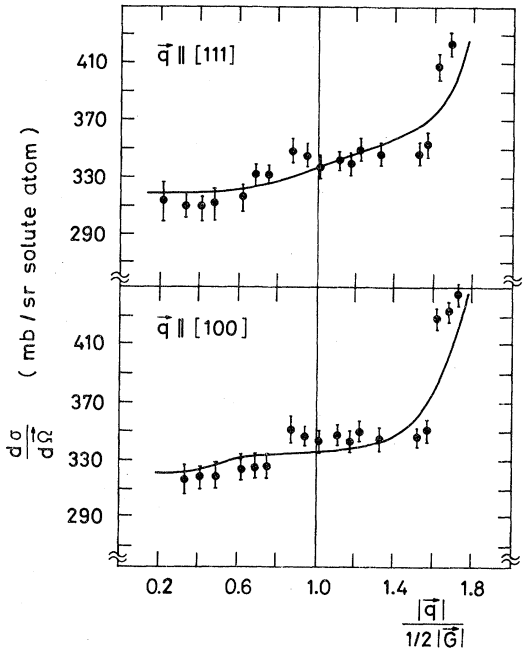

FIG. 5. Neutron cross section for the [100] and [111] directions. Of the theoretical curves only those in TW approximation are plotted; the hatched strips have the same meaning as in Fig. 4.

present scattering experiment. In Figs. 4 and 5 these limits, predicted by independent experiments,[1,2] are indicated by the hatched strips at $\vec{q}=0$. We see that our scattering experiment reproduces well the $\vec{q}=0$ limit. The most pronounced structure in the cross section appears in the close-packed [110] direction, and this structure is fairly well described by the theoretical model. The agreement between theory and experiment is reasonable also for the [100] and the [111] directions, as seen in Fig. 5, though the fine structure of the observed cross section is somewhat less well reproduced, especially along the [111] axis.

The theoretical curves are obtained by using Eqs. (15a)–(15c) with both $g_{\alpha\beta}$ and $F(\vec{k})$ calculated in the linear screening approximation [Eq. (36)]. As we have emphasized, this gives us $\vec{u}(\vec{q})$ and $K(\vec{q})$ within a given accuracy $\sim(\vec{v}_{\vec{G}}/E_F)^2$ for a general $\vec{q}$, but with a smaller accuracy for $\vec{q} \ll \vec{G}$. We can find, however, the theoretical value for $K(\vec{q}=0)$ *within* the above accuracy via ΔE_{per} by Eqs. (51) and (50) by calculating Δp, and *the difference is precisely the contribution of the third- and fourth-order terms to* $F(\vec{k})$ (for the TW curve, also see the remark above). The accurate re-

for each screening approximation. As predictable from the results of Table II, the nonlinear screening terms change $K(\vec{q})$ and thereby the scattering intensity quite appreciably for small $\vec{q}$'s. The error at $|\vec{q}| \sim 0$ for the TW curve is still moderate, as compared to the GV curve, the shape of which is being changed completely near $\vec{q}=0$ by the contributions $F^{(3)}$ and $F^{(4)}$. In order to see in detail how the influence of the nonlinear screening

TABLE III. Effect of the nonlinear screening in the scattering amplitude $K(\vec{q}\to 0)$, with $\vec{q} \parallel [110]$. In the first row both c_l^2 and Δp in Eq. (50) were calculated by the method of long waves (LW), keeping only linear screening terms. In the second row c_l^2 is obtained by the method of homogeneous deformations (HD), and in the third row both c_l^2 and Δp are calculated in this way. The notation for Δp is that of Table II; the experimental value is based on $(\Delta\Omega_0/\Omega_0)_{\text{expt}}$.

Sound velocity c_l^2	Impurity pressure Δp	$K(\vec{q}\to 0)$ TW	$K(\vec{q}\to 0)$ GV	$\frac{d\sigma}{d\Omega}$ (mb) TW	$\frac{d\sigma}{d\Omega}$ (mb) GV
LW	$[\Delta p]_F$	+0.028	−0.020	322.9	342.0
HD	$[\Delta p]_F$	+0.030	−0.019	322.1	341.6
HD	Δp	+0.011	+0.040	329.6	318.2
Experiment		0.032 ± 0.003[a]		321 ± 1.5[a]	
		0.017 ± 0.003[b]		327 ± 1.5[b]	

[a] Reference 1.
[b] Reference 2.

terms appears *progressively* in the scattering pattern, we ought to recalculate the continuous curves with including the contributions of $F^{(3)}$ and $F^{(4)}$ at a general argument. Following these curves up to $\vec{q}=0$ [and correcting, for the TW curve, $P(\vec{q})$ so as to satisfy *exactly* Eq. (22)], we would arrive at the values indicated by the arrows in Fig. 4. We did not proceed so because of the rather complicated form of the polarization functions $\Lambda^{(3)}$ and $\Lambda^{(4)}$, but we obtain a quantitative result there where the effect is certainly the largest: at the point $\vec{q}=0$.

Besides the nonlinear screening part of $F(\vec{q})$, there is a second reason why the curves of Fig. 4 do not arrive at the points indicated by the arrows, though quantitatively this effect is much less important. We refer to the fact[6] that nonlinear screening contributions appear also in the calculation of phonon frequencies and thus of $g_{\alpha\beta}(\vec{q})$ for small $\vec{q}$'s. As a consequence, the longitudinal sound velocities obtained by the method of long waves differ from their correct values as calculated by the method of homogeneous deformations.[6] Now, the *curves* in Fig. 4 have been calculated in linear screening approximation for both $F(\vec{k})$ and $g_{\alpha\beta}(\vec{q})$ for all wave vectors, while for the *points at* $\vec{q}=0$ indicated by the arrows both $F(\vec{k})$ and the sound velocities have been determined from the energy of a homogeneously deformed crystal, thus consequently in the accuracy $(\tilde{v}_{\vec{G}}/E_F)^2$. We show now that, quantitatively, the dominant effect for the lattice strain comes from $F^{(3)}$ and $F^{(4)}$. In the second row of Table III we exhibit $K(\vec{q}=0)$ as calculated by the method of homogeneous deformations for the sound velocities but neglecting $F^{(3)}$ and $F^{(4)}$. The numbers show that the difference due to improving the method to calculate the sound velocities does not significantly modify the result, whereas the contributions of $F^{(3)}$ and $F^{(4)}$ changes the magnitude of K substantially in both cases, altering even its sign for the GV screening approximation.

Having calculated the strain field in $\vec{q}$ space, according to Eq. (15), we can apply the transformation Eq. (13) to have the real displacements in different crystallographic directions. The integration in BZ was performed by a method[29] due to Miller using a cubic mesh in the irreducible part of the zone, as was done previously for the alkali alloys.[10] The finest mesh consisted of 60 cubes in the $\frac{1}{48}$th irreducible part of the BZ, implying 60×27 integration points in this polyhedron. The results for the nearest shells are shown in Table IV. We see that even for the nearest neighbors the displacements are of the order of $\sim 10^{-3}a$, justifying *"a posteriori"* the neglect in Eq. (9) of the linear terms in $\vec{u}$ and explaining the smallness of

TABLE IV. Radial displacements around an Li atom in Al solvent in units of the lattice constant a. The third column is the value for an isotropic elastic medium with B and c_{44} of pure Al and with the experimental value for $\Delta\Omega_0/\Omega_0$ [Eqs. (17) and (42) with $\vec{A}=\hat{l}B/c_{44}$)]. The results for the TW screening approximation are shown.

Neighbor	$\frac{\vec{u}\hat{l}}{a}$	Isotropic elastic continuum
(110)	−0.001 2	−0.0015
(200)	−0.001 4	−0.0007
(220)	−0.000 8	−0.0004
(222)	−0.000 02	−0.0002
(400)	+0.000 1	−0.0002
(330)	−0.000 2	−0.0002

the energy of relaxation and its derivatives. In fact, the calculation of $\vec{f}(\vec{l})$ and $h_{\vec{l}\alpha\vec{l}'\alpha'}$ by Eqs. (8), (14), (38), and (39) together with the tabulated values for the displacements gives that the term neglected in Eq. (9) contributes less than 1%, 1.7%, 4.5%, and 0.1%, respectively, for the first four neighboring shells around the solute atom.

C. The heat of solution

The energy needed to dissolve one impurity atom is obviously the difference in total energy of the alloy and of its separate components,

$$\Delta H_s=\lim_{c=0}\frac{1}{c}[E(\text{alloy},\Omega_0,\bar{Z}) - (1-c)E_h(Z,\Omega_{0h})-cE_i(Z^*,\Omega_{0i})]. \tag{52}$$

This quantity is also called the limiting partial heat of mixing at $T=0$. By using Eqs. (6) and (37) we get in a straightforward fashion

$$\Delta H_s=\Delta H_{\text{VP}}+\Delta H_{\text{EL}}+\Delta H_{\text{es}}+\Delta H_{\text{av}} + \Delta H_n+(\Delta H_{\text{pot}}+\Delta E_{\text{rel}}), \tag{53}$$

where

$$\Delta H_{\text{VP}}=E_i(Z^*,\Omega_0)-E_i(Z^*,\Omega_{0i}) \tag{54}$$

is the energy invested to "prepare" the volume (and crystal structure) for the impurity atom[8] having initially $\Omega=\Omega_{0i}$ in its pure phase and dissolved in a lattice with $\Omega=\Omega_0$, and

$$\Delta H_{\text{EL}}=Z^*[\epsilon_0(r_{s0})-\epsilon_0(r^*_{s0})]-\Delta Z\,\frac{r_{s0}}{3}\left(\frac{d\epsilon_0}{dr_{s0}}\right) \tag{55}$$

is the variation of the electron-liquid energy due to the difference in valence. The notation is $(4\pi/3)r^{*3}_{s0}=\Omega_0/Z^*$. The contributions

$$\Delta H_{\text{es}}=\tfrac{1}{2}e^2\frac{(\Delta Z)^2}{R_a}\gamma \tag{56}$$

and

$$\Delta H_{av} = -\frac{\Delta\beta \Delta Z}{\Omega_0} \tag{57}$$

come from the change in the Madelung and the average potential-energy terms, and

$$\Delta H_n = \frac{\Delta Z}{\Omega_0}\frac{\partial}{\partial n_0}\left\{-\tfrac{1}{2}\sum_{\vec{G}} |v_{\vec{G}}|^2 \Omega_0 \frac{P_{\vec{G}}}{\epsilon_{\vec{G}}}\right\} + \tfrac{1}{2}\sum_{\vec{G}} |v^*_{\vec{G}}|^2 \Omega_0 \left[\left(\frac{P_{\vec{G}}}{\epsilon_{\vec{G}}}\right)_{r^*_{s0}} - \left(\frac{P_{\vec{G}}}{\epsilon_{\vec{G}}}\right)_{r_{s0}}\right] \tag{58}$$

arises from $E^{(2)}$. The above terms, except for the "volume-preparation" energy Eq. (54), disappear for a homovalent impurity, whereas the contribution

$$\Delta H_{pot} + \Delta E_{rel} = \tfrac{1}{2}\sum_{\vec{G}} |\Delta v_{\vec{G}}|^2 \Omega_0 \frac{P_{\vec{G}}}{\epsilon_{\vec{G}}} - \frac{1}{2}\frac{1}{N}\sum_{\vec{q}} |\Delta v_{\vec{q}}|^2 \Omega_0 \frac{P_{\vec{q}}}{\epsilon_{\vec{q}}} + \Delta E_{rel} \tag{59}$$

is present in both the homovalent and heterovalent cases. In the particular case of *Al*Li the numerical results for the individual terms in Eq. (53) are shown in Table V.

As in the case of the volume change, we see again the large positive contribution (of several rydbergs) representing the investment in the electrostatic energy. This is compensated by ΔH_{pot} and by the electron liquid and average potential terms, the net result being of some mRy. The large contribution of ΔH_{pot} originates in the integral over $\vec{q}$, since for $Z^* \neq Z$ the integrand gets large near $\vec{q} = 0$. For experimental data to compare with, we have the heat of solution for the liquid alloy[30] which is of the same order of magnitude, though negative. In view of the fact that the heat of solution for a disordered solid solution is expected to be somewhat more positive than for the liquid, the calculated result is not unreasonable.

V. CONCLUSIONS

The consistency of the pseudopotential theory for the calculation of the lattice strain around a heterovalent solute atom has been demonstrated. Since the polarization of the electron liquid gives rise to complicated many-body interaction among the ions and even the "pair forces" of the linear screening approximation depend, via the dielectric function, in an intricate way on the volume, the calculation of the strain field in the dilute alloy was seen to be problematic even for a homovalent impurity.[9] It has been shown here that, independently of the valency of the solute atom, the volume change per solute atom on the one hand, and the strain field for not "too small" wave vectors on the other hand, can consistently be found, within the accuracy of $(v_{\vec{G}}/E_F)^2$, by the linear screening approximation, but for $0 < |\Delta\vec{q}| \ll |\vec{G}|$ there is a contribution from higher-order polarization into the distorting force and, thereby, the displacement field, which has also to be retained. The difference in the results for the heterovalent and homovalent impurity is substantial: For $Z^* \neq Z$ both third- and fourth-order polarization contribute, on equal footing with the linear screening term, to build up the preasymptotic and asymptotic lattice strain, whereas for $Z^* = Z$ the third-order term simplifies and the fourth-order term is completely absent at the above accuracy. The stronger effect of nonlinear screening in the case of a heterovalent solute is, of course, plausible, in view of the much stronger perturbation of the system.

The application of the theory to the dilute *Al*Li alloy illustrates well these points. First, the volume change and the observed neutron scattering pattern could reasonably well be predicted, and second, a spectacular change in the calculated scattering curves occurs on taking into account or neglecting the nonlinear screening part of the asymptotic displacement amplitude. In calculating the volume change per impurity for this alloy we find a balance between the large non-bonding contributions to the energy and to the internal pressure, associated with the Madelung energy, and the strong bonding term coming from the energy of the homogeneous electron liquid. This bonding term arises since the electron liquid is in a rather compressed state in pure aluminium, thus dissolving lithium with one itinerant

TABLE V. Energy contributions to the heat of solution for *Al*Li, Eq. (53) in Ry. The terms in the first four columns would disappear for $Z^* = Z$. The experimental value is known only for the liquid (Ref. 30) solution.

ΔH_{EL}	ΔH_{es}	Contributions	ΔH_{av}	ΔH_n	ΔH_{VP}	ΔH_{pot}	ΔE_{rel}	ΔH_s	Total ΔH_s(expt.) liquid
−0.2522	2.4053	TW	−0.4506	0.0201	0.0046	−1.7122	−0.000 03	0.015	−0.010
		GV	−0.4006	0.0141	0.0046	−1.7447	−0.000 1	0.026	

electron in the same atomic sphere is quite accomodating. Polarization terms slightly tilt this balance over to a negative pressure. We believe that the "anomalous" contraction of the Al-Li system can now be considered as quantitatively understood. The result for the heat of solution at 0 K is of the observed magnitude of about 10 mRy, but the calculated value has a positive sign whereas the experimental value, for a liquid alloy, is negative. Even if we know that the disordered solid solution has a somewhat more positive heat of solution than the liquid, this result cannot yet be considered as very satisfactory. The problem is, of course, in the nearly zero value of this quantity, as compared to the energy terms by which it is obtained.

It is reassuring that the present diffuse elastic scattering data are in good agreement with the other experimental information on the volume change in *Al*Li. Indeed, the limiting value of the measured cross section in the [110] direction is 325 ± 5 mb/sr per solute atom, as seen in Fig. 4, and this corresponds, via Eqs. (3) and (51), to $\Delta a/ac = -0.012 \pm 0.006$. The agreement between the calculated and experimental scattering patterns is quite good in the [110] direction (Fig. 4) and fairly reasonable also for the [100] and [111] directions, the only appreciable difference appearing in the structure near the zone boundary along the [111] axis. The reason for this difference is not clear, but the overall description of the scattering even in the [111] direction can be considered as acceptable. As a whole, the numerical results suggest that the present method of using "pure-metal" potentials to describe the alloy may work reasonably well for dilute solid solutions of two *sp* metals.

An overall characteristic of the numerical calculation is the strong cancellation of the large electrostatic and pseudopotential terms, a known and omnipresent difficulty in the pseudopotential method for either the pure polyvalent metals or their alloys. To this one has to add that the use of only the lowest order $[\sim(v_{\vec{G}}/E_F)^2]$ structure-dependent terms in the series expansion for ΔE_{per} is a serious approximation, in particular, for a heterovalent alloy. Hence, the question arises if the agreement with, for example, the observed volume change, is not fortuitous. In fact, by using somewhat different parameters in our model potential (e.g., those with R_c and λ outside the "physical range" of the core radius but still reproducing the pure-metal cohesive parameters) the agreement with experiment is less satisfactory. This high sensitivity of the result for both the volume change and the scattering intensity to the form of the potentials means, however, that the description of the alloying process is a good test for a proposed ion-electron model potential. We consider as encouraging to observe that the "best" of our pure-metal potentials has led, indeed, to the best calculated numbers for the alloy.

ACKNOWLEDGMENTS

We thank Miss Regina Dunkmann for preparing the crystals and for her assistance during the measurements. The support of the Swiss National Science Foundation through Grant No. 2.312-079 is gratefully acknowledged.

APPENDIX

In order to prove Eqs. (40a)–(40d) we proceed by adapting the method of Brovman and Kagan[6] worked out for treating the long wave expansion of the dynamical matrix of pure metals. For a general term $n>2$ in Eq. (18) we have, analogously to the case of a pure solvent,

$$E^{(n)} = \Omega_0 \sum_{\vec{q}_1} \times \cdots \times \sum_{\vec{q}_n} \frac{\Lambda^{(n)}(\vec{q}_1 \times \cdots \times \vec{q}_n)}{\epsilon_{\vec{q}_1} \times \cdots \times \epsilon_{\vec{q}_n}} \times f_{\vec{q}_1} \times \cdots \times f_{\vec{q}_n} \times \Delta(\vec{q}_1 + \cdots + \vec{q}_n), \quad \text{(A1)}$$

where $\Lambda^{(n)}$ is the "irreducible" multipole polarization function[6] for the electron liquid, $f_{\vec{q}}$ is given by Eq. (23a) and the function Δ ensures momentum conservation. Taking the coefficient of $\vec{u}(\vec{l})$ in the expansion of Eq. (A1) in terms of the displacements, we arrive at

$$F^{(3)}(\vec{k}) = 6\Omega_0 \frac{v_{\vec{k}}}{\epsilon_{\vec{k}}} \left(\tfrac{1}{2} \sum_{\vec{q}} \Lambda^{(3)}_{\vec{k},\vec{q},-\vec{k}-\vec{q}} \frac{1}{N} \frac{\Delta v_{\vec{q}}}{\epsilon_{\vec{q}}} \frac{\Delta v_{-\vec{k}-\vec{q}}}{\epsilon_{-\vec{k}-\vec{q}}} + \sum_{\vec{G}'} \Lambda^{(3)}_{\vec{k},\vec{G}',-\vec{k}-\vec{G}'} \frac{v_{\vec{G}'}}{\epsilon_{\vec{G}'}} \frac{\Delta v_{-\vec{k}-\vec{G}'}}{\epsilon_{-\vec{k}-\vec{G}'}} \right) \quad \text{(A2)}$$

and

$$F^{(4)}(\vec{k}) = 12\Omega_0 \frac{v_{\vec{k}}}{\epsilon_{\vec{k}}} \sum_{\vec{G}} \sum_{\vec{G}'} \Lambda^{(4)}_{\vec{k},-\vec{k}-\vec{G}-\vec{G}',\vec{G},\vec{G}'} \frac{\Delta v_{-\vec{k}-\vec{G}-\vec{G}'}}{\epsilon_{-\vec{k}-\vec{G}-\vec{G}'}} \times \frac{v_{\vec{G}}}{\epsilon_{\vec{G}}} \frac{v_{\vec{G}'}}{\epsilon_{\vec{G}'}} + \cdots . \quad \text{(A3)}$$

In Eq. (A3) only the main term is written. These expressions, of the order $\sim(\tilde{v}_{\vec{q}}/E_F)^n$ $(n=3,4)$ for a *general* $\vec{k}$, become of the order $\sim(\tilde{v}_{\vec{G}}/E_F)^2$ for $\vec{k} \to 0$ or $\vec{k} \to \vec{g}$. To see this, we will make use of the identities[6]

$$\frac{\Lambda^{(3)}_{0,\vec{G},-\vec{G}}}{(\epsilon_{\vec{G}})^2} = \frac{P_0}{6} \frac{d}{dn_0} \left(\frac{P_{\vec{G}}}{\epsilon_{\vec{G}}} \right), \quad \text{(A4)}$$

$$\frac{\Lambda^{(4)}_{0,0,\vec{G},-\vec{G}}}{(\epsilon_{\vec{G}})^2} = -\frac{P_0^2}{24}\frac{d^2}{dn_0^2}\left(\frac{P_{\vec{G}}}{\epsilon_{\vec{G}}}\right), \tag{A5}$$

and

$$\frac{\partial}{\partial q_\alpha}(\Lambda^{(3)}_{\vec{q},-\vec{q},-\vec{G},\vec{G}})_{\vec{q}=0} = \frac{1}{2}\frac{\partial}{\partial G_\alpha}(\Lambda^{(3)}_{0,\vec{G},-\vec{G}}). \tag{A6}$$

From Eq. (A2) we arrive immediately at Eq. (40a), by using Eq. (A4), as shown already for the case of homovalent alloys.[9] We have the largest terms in the sum of Eq. (A3) at $\vec{G} = -\vec{G}$, with $\Lambda^{(n)}_{\vec{k},-\vec{k},\vec{G},-\vec{G}}$ as coefficients, which are easily transformed into Eq. (40d) by using Eq. (A5). At $\vec{k} \to \vec{G}$ we have a large term again at $\vec{G}' = -\vec{G}$ in the second sum of Eq. (A2), leading to Eq. (40b), and a similar selection of terms leads to Eq. (40c) via Eq. (A6).

[1] H. J. Axon and W. Hume-Rothery, Proc. R. Soc. London Ser. A 193, 1 (1948).
[2] E. D. Levine and E. J. Rappaport, Trans. AIME 227, 1204 (1963).
[3] M. A. Krivoglaz, *Theory of X-Ray and Thermal Neutron Scattering by Real Crystals* (Plenum, New York, 1969).
[4] G. S. Bauer, in *Treatise on Materials Science and Technology*, edited by H. Herman (Academic, New York, 1979), Vol. 15.
[5] V. Heine and D. Weaire, in *Solid State Physics*, edited by F. Seitz, D. Turnbull, and H. Ehrenreich (Academic, New York, 1970), Vol. 24.
[6] E. G. Brovman and Yu. M. Kagan, in *Dynamical Properties of Solids*, edited by G. K. Horton and A. A. Maradudin (North-Holland, Amsterdam, 1974), Vol. 1.
[7] Z. Popovic, J. P. Carbotte, and G. R. Piercy, J. Phys. F 3, 1008 (1973).
[8] G. Solt and A. P. Zhernov, Solid State Commun. 23, 759 (1977).
[9] G. Solt, Phys. Rev. B 18, 720 (1978).
[10] G. Solt and A. P. Zhernov, J. Phys. F 9, 1013 (1979).
[11] K. Werner, W. Schmatz, G. S. Bauer, E. Seitz, H. J. Fenzl, and A. Baratoff, J. Phys. F 8, L207 (1978).
[12] *Metals Handbook*, 8th ed., Vol. 8 of *Metallography Structures and Phase Diagrams* (Am. Soc. for Metals, Metals Park, 1973).
[13] C. G. Shull, *Table of Coherent Neutron Scattering Amplitudes* (MIT, Cambridge, Mass., 1972).
[14] W. J. Pfann, *Zone Melting* (Wiley, New York, 1966).
[15] H. Glätli (private communication).
[16] K. Werner, thesis, Jülich Report No. 1519, 1978; unpublished.
[17] F. Toigo and T. O. Woodruff, Phys. Rev. B 2, 3958 (1970).
[18] D. J. W. Geldart and S. H. Vosko, Can. J. Phys. 44, 2137 (1966).
[19] D. Pines and P. Nozières, *The Theory of Quantum Liquids* (Benjamin, New York, 1966), Vol. 1.
[20] Z. Popovic, J. P. Carbotte and G. R. Piercy, J. Phys. F 4, 351 (1974).
[21] P. S. Ho, Phys. Rev. B 3, 4035 (1971).
[22] D. E. Temkin, Fiz. Tverd. Tela (Leningrad) 11, 2002 (1969) [Sov. Phys.—Solid State 11, 1614 (1970)].
[23] M. W. Finnis and M. Sachdev, J. Phys. F 6, 965 (1976).
[24] G. Solt and A. P. Zhernov, *Proceedings of the 7th Symposium on Electronic Structure of Metals and Alloys, Gaussig (GDR), 1977* (Technishe Universität, Dresden, 1977); A. P. Zhernov and G. Solt, Fiz. Tverd. Tela (Leningrad) 21, 3048 (1979) [Sov. Phys.—Solid State 21, 1754 (1979)].
[25] V. G. Vaks and A. V. Trefilov, Fiz. Tverd. Tela (Leningrad) 19, 244 (1977) [Sov. Phys.—Solid State 19, 139 (1977)].
[26] N. W. Ashcroft and D. C. Langreth, Phys. Rev. 155, 682 (1967).
[27] D. D. Ling and C. D. Gelatt, Jr., Phys. Rev. B 22, 557 (1980).
[28] J. Friedel, Philos. Mag. 46, 514 (1955).
[29] J. C. P. Miller, Math. Computation (MTAC) 14, 130 (1960).
[30] A. R. Miedema, P. F. de Châtel, and F. R. de Boer, Physica 100B, 1 (1980).